Engineering Structures 303 (2024) 117556

Contents lists available at ScienceDirect

Engineering Structures

journal homepage: www.elsevier.com/locate/engstruct

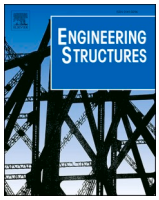

# Parametric analysis of post-earthquake fire resistance of reinforced concrete frames without seismic design

Hugo Vitorino, Paulo Vila Real, Carlos Couto, Hugo Rodrigues *

*RISCO, Civil Engineering Departament, University of Aveiro, Aveiro, Portugal*

ARTICLE INFO

*Keywords:*
Post-earthquake fire
Earthquake damage
Fire resistance
Parametric fire curves
Reinforced concrete
Numerical analysis

ABSTRACT

To gain a deeper understanding of post-earthquake fire behaviour, 100 reinforced concrete (RC) frames representative of a building stock designed without considering seismic loading were modelled using the software SAFIR. A total of 4400 numerical analyses were performed to investigate the impact of different assumptions, such as the type of damage, damage location, number of sides of the RC elements exposed to fire, location of the fire and different fire curves on the post-earthquake fire resistance of the RC frames. Results showed that heavily damaged frames have significantly lower fire resistance compared to undamaged frames. Variations in the number of heated sides and fire locations were found to lead to significant differences in the time until the collapse of the RC frames. Moreover, due to increased demand for assistance following a large earthquake, rescue teams are likely to experience prolonged response times, exacerbating the potential for loss of life and infrastructure. Assuming parametric fire curves without firefighting efforts is a reasonable approach in post-earthquake events. This approach led to quicker collapse times compared to the standard fire curve ISO 834. This aspect combined with a lower fire resistance of the damaged structures can ultimately lead to the loss of lives and infrastructures. Therefore, a comprehensive understanding of post-earthquake fire behaviour becomes crucial for developing recommendations that can ensure the safety of RC structures in such events.

## 1. Introduction

Earthquake shaking has the potential to generate ignitions that, in some cases, evolve into major fires and even conflagrations, which can cause more damage and have a worse impact than the earthquake itself, as was observed in the 1906 San Franscisco and the 1923 Kanto earthquakes [1]. The fire outbreaks in these earthquakes were mainly related to the breaking of electrical wiring due to structural damage in buildings and the overturning of heat sources, such as stoves, kerosene lamps, heaters and cookers [1–4]. After an earthquake, delays in firefighting response may occur due to communication failures and blocked streets. Simultaneous occurrence of several fires can also contribute to an ineffective response [1,5,6].

The damage in buildings caused by earthquake can lead to the loss of reliability of active and passive fire protection systems. The malfunctioning of active fire protection systems (detection, alarm, and suppression systems) makes them unreliable, leading to undetected ignitions that can cause large fires that will be more difficult to extinguish. Passive fire protection systems can also be damaged. Broken windows can increase ventilation in compartment fires, leading to more severe fire scenarios [1,6]. Adequate water supplies are crucial to stop the fire spread, but water distribution systems may be compromised due to their expected failure after an earthquake [1,7]. The combination of these aspects can decrease the probability of immediate extinguishment of the fire. There are several numerical studies where it is applied a sequential analysis approach to consider the effect of earthquake and fire to study the post-earthquake fire phenomenon in RC structures. The approach has three steps, the first deals with the application of the gravity loads that are static and uniform, the second corresponds to the application of a pseudo earthquake load (pushover) and the last step is related to the fire loads on structures [8–12]. These numerical studies indicate that structures significantly damaged by earthquakes have lower fire resistance compared to undamaged structures [10]. For instance, in [13–15], the time until the collapse of a heavily damaged frame was reported to be over two hours less than that of an intact frame, highlighting the impact of the seismic damage on the fire resistance of structures. Experimental studies showed that a significant reduction in the concrete cover of structural elements leads to faster heat

* Corresponding author.
*E-mail addresses:* hugo.vitorino@ua.pt (H. Vitorino), pvreal@ua.pt (P. Vila Real), ccouto@ua.pt (C. Couto), hrodrigues@ua.pt (H. Rodrigues).

https://doi.org/10.1016/j.engstruct.2024.117556
Received 24 April 2023; Received in revised form 11 January 2024; Accepted 19 January 2024

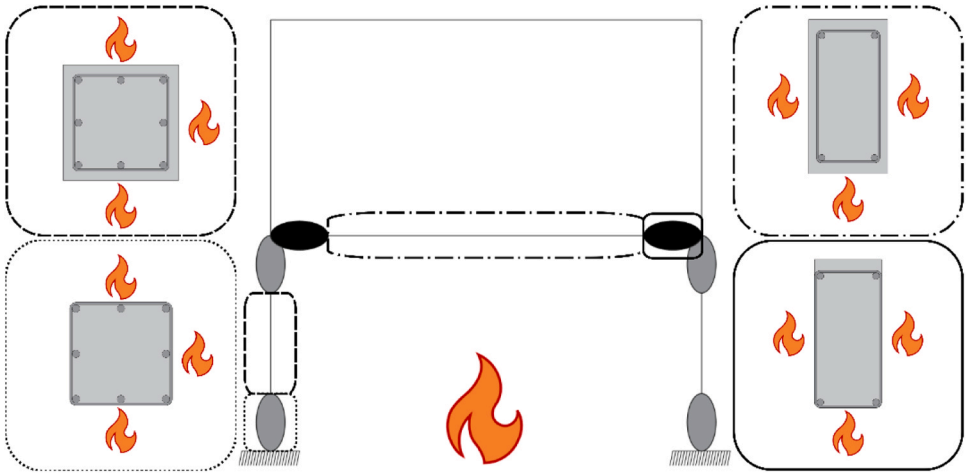

**Fig. 1.** Schematic of the modelling strategy.

penetration [16]. Several experimental studies investigating the impact of post-earthquake fires on RC frames have highlighted that the position of openings in compartments and the resulting movement of fire plumes and hot gases significantly influence the temperature evolution in structural elements [17–20]. Additionally, the location of the fire may or may not overlap with the locations of the damage resulting from the seismic action [17]. It was also observed that ductile detailing leads to better performance of the RC frames, which indicates that the common recommendations for the seismic design are also beneficial for the fire resistance of the RC structures [17,20].

The main objectives of the present work were to identify the impact of the type and location of damage, the influence of the number of heated sides, and the location and type of fire on the fire resistance of RC frames.

It is important to note that, to achieve these objectives, frames representing a specific building stock were developed. Consequently, this contributes to a comprehensive understanding of the post-earthquake fire resistance of a specific urban area, not just a particular building. These studies are relevant due to the scarcity of research analysing the post-earthquake fire resistance of a specific build stock. Furthermore, different types of fire curves were applied and compared, adding a relevant aspect to the study.

The results provide a better comprehension of the post-earthquake fire phenomenon and can be crucial for developing recommendations that ensure a safer performance of RC structures in such events.

## 2. Simplified methodology for post-earthquake fire assessment of RC frames

### 2.1. Numerical modelling assumptions

The numerical analyses to investigate the post-earthquake fire resistance of RC frames were developed using the SAFIR software [21], [22]. In SAFIR, it is possible to perform analyses of structures under elevated and ambient temperatures. The thermal and mechanical analysis are calculated separately and subsequently, where the temperature

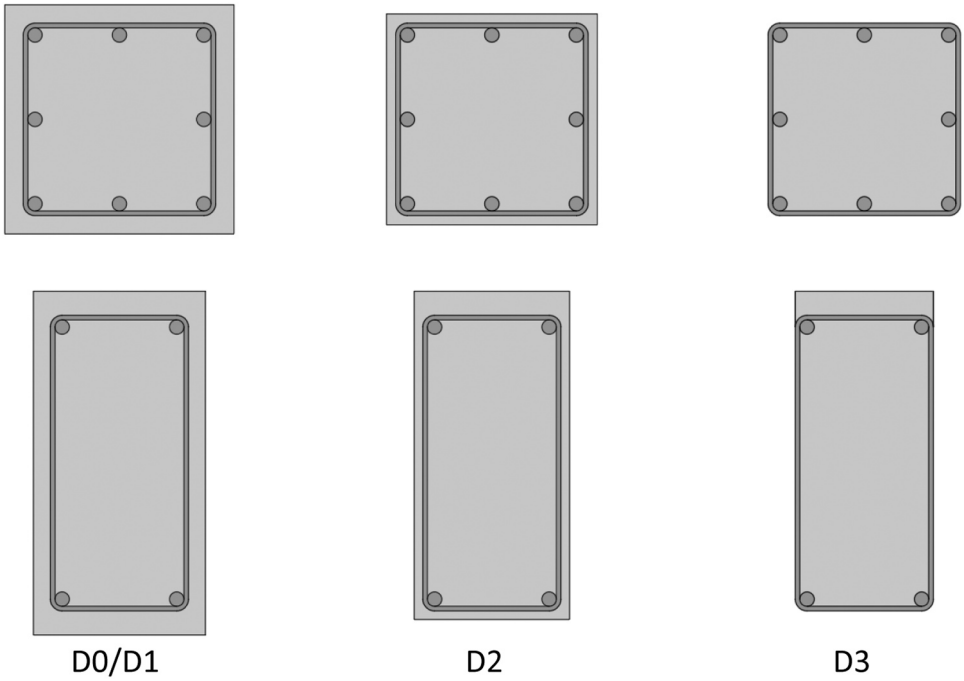


**Fig. 2.** Schematic of the sections of the columns and beams considered in the analyses.

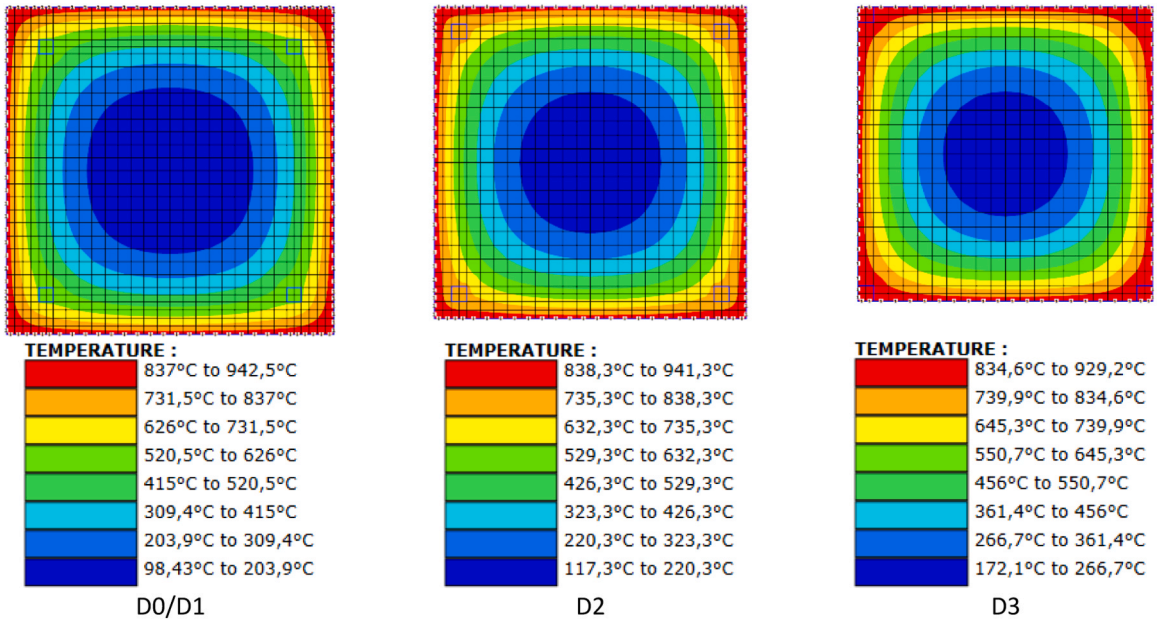


**Fig. 3.** Temperature profiles of a column with the fire curve ISO 834 with damage D0/D1, D2 and D3 after one hour.

distribution has a great influence on the mechanical response [21], [22]. The constitutive models of concrete and steel materials defined in SAFIR are based on the recommendations from Eurocode 2 (EN 1992–1-2) [23]. Concrete input parameters include aggregate type (siliceous or calcareous), specific mass of dry concrete, free water content, a parameter for tuning thermal conductivity between the upper limit and the lower limit, Poisson's ratio, and compressive and tensile strength [22], [23]. The reinforcement steel model is based on the Eurocode 2, with input parameters including Young modulus, Poisson's ratio, and yield strength [22], [23]. Cross-section geometry is defined with a fibre model, where each fibre can have a different material, allowing for the creation of composite sections, e.g. reinforced concrete [22], [24]. The temperature distribution of the element cross-section is obtained through a 2D analysis, considering heat transfer by conduction according to the Fourier law. Structural behaviour is determined by geometry, support conditions, loads, strength of the materials, and the effect of the temperature. The numerical analysis stops if no convergence is obtained, at a time defined by the user, or if a numerical problem is found at the

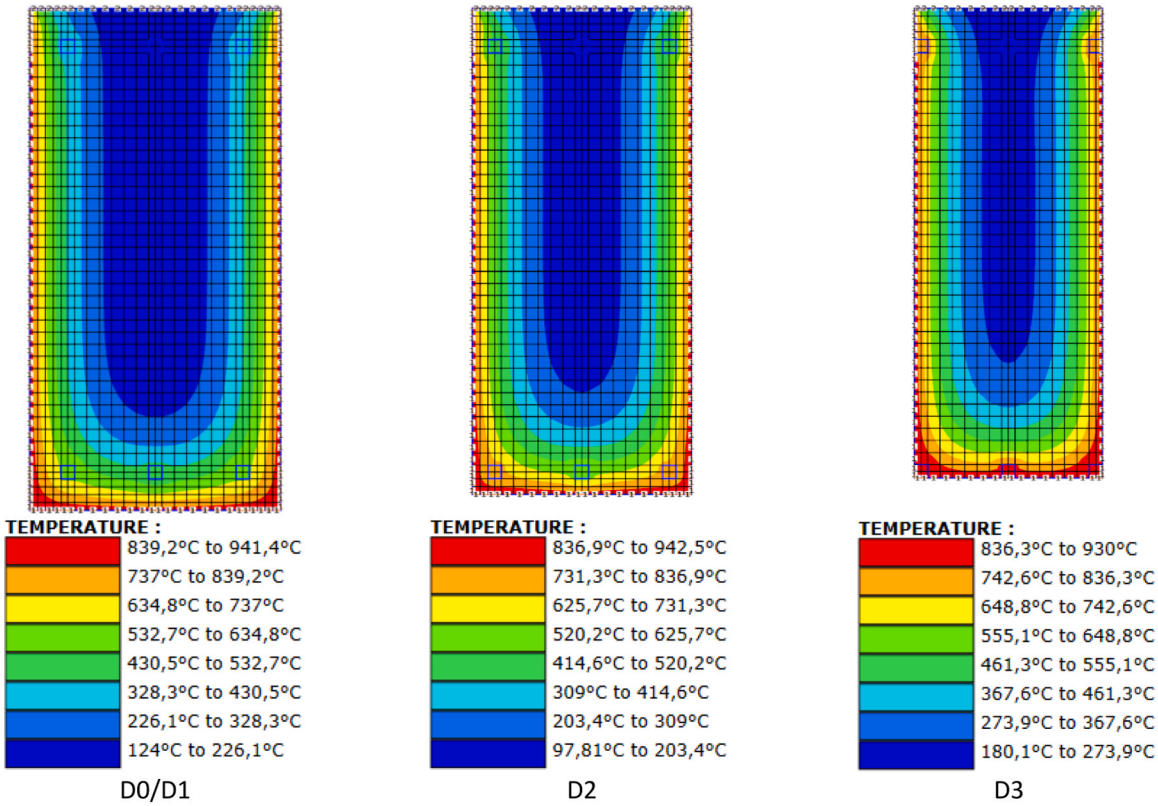


**Fig. 4.** Temperature profiles of a beam with the fire curve ISO 834 with damage D0/D1, D2 and D3 after one hour.

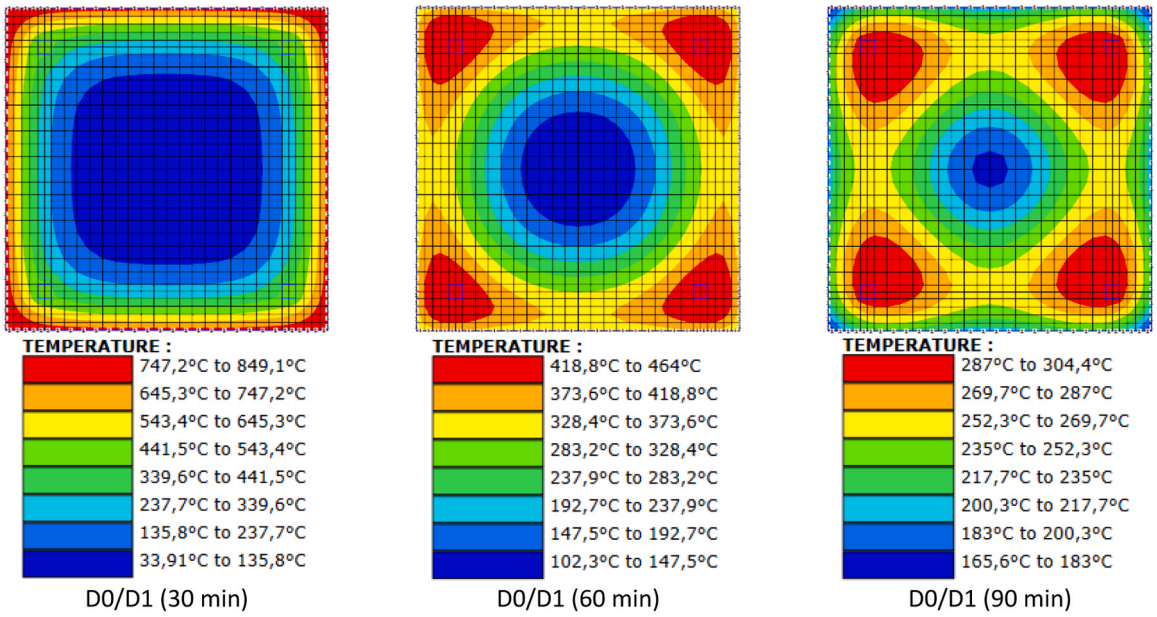


**Fig. 5.** Temperature profiles of a column with a parametric fire curve, with damage D0/D1 at 30, 60 and 90 min.

material level [24], [25]. The numerical modelling strategy involves developing columns and beam sections with different types of damage and fire, which are later incorporated into frames with various characteristics. The time until the collapse of these frames is then analysed and compared. A schematic of the modelling strategy is represented in Fig. 1. The schematic represents a one-bay and two-floor frame that has damage and fire on the bottom floor. In this specific example, columns and beams have fire on three sides, and the damaged sections are located near the supports and near the beam-to-column regions.

### 2.2. Seismic damage

To simulate the seismic damage induced by the earthquake, a reduction of the concrete cover in the RC elements (columns and beams) in the plastic hinge zone was considered. This simplified approach follows the same strategy adopted in [8–12], [26]. The seismic damage was represented by three types of damage, namely, damage D0/D1, D2 and D3. Damage D0/D1 represents an undamaged section (D0) and a section with minor cracks (D1). Damage D2 represents a section with concrete

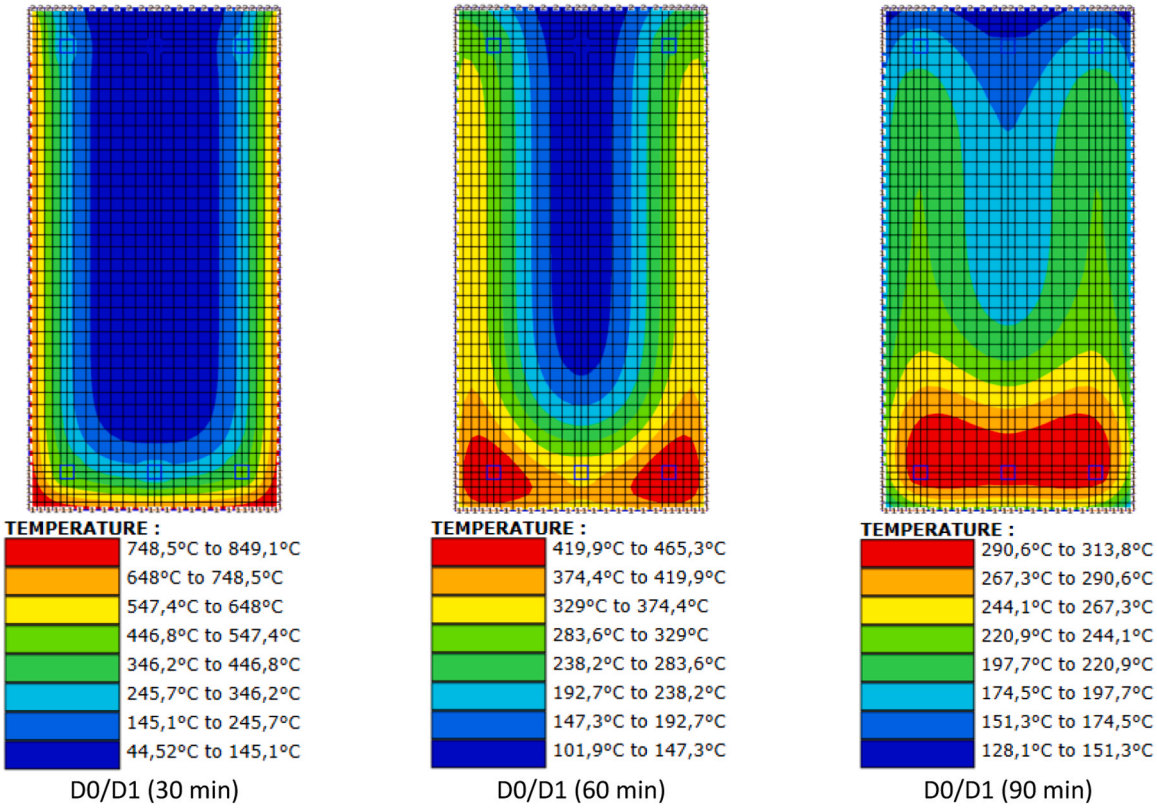


**Fig. 6.** Temperature profiles of a beam with a parametric fire curve, with damage D0/D1 at 30, 60 and 90 min.

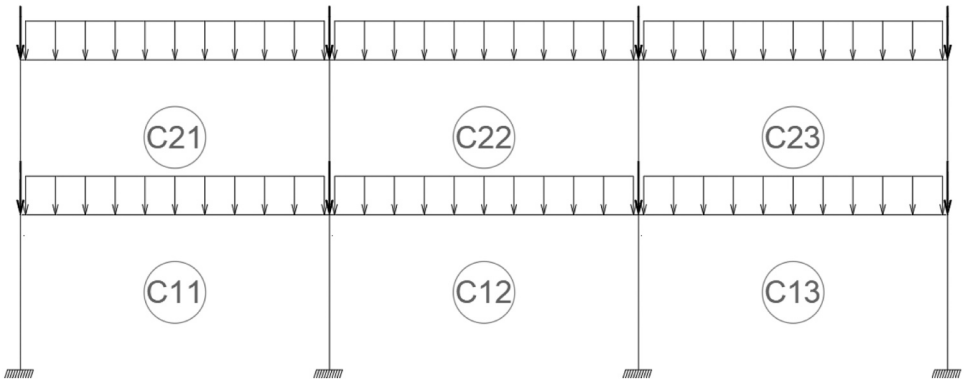


**Fig. 7.** Typology of the frame developed in the parametric study.

spalling, involving the removal of the exterior fibres (equivalent to a 50% reduction of the section cover) and damage D3 represents a severely damaged section that is simulated by the removal of the entire section cover, leaving the longitudinal steel reinforcement exposed. Based on the state-of-the-art, minor cracks do not significantly influence the thermal evolution through concrete, which means that considering the same model to represent damage D0 and D1 can be an acceptable approach [27], [28]. The types of damage represented in the numerical analyses were based on the definitions of the damage states in FEMA 356 [29]. Damage D0/D1, D2 and D3 intend to correspond, respectively, to Immediate Occupancy (IO), Life Safety (LS) and Collapse Prevention (CP). The IO level corresponds to minor damage in the structural elements; LS level corresponds to spalling and shear cracking for ductile columns and extensive damage to beams; and CP level corresponds to extensive spalling in the columns and beams [11], [26], [29]. In the columns, damage is considered on all sides of the cross-section, while in beams, damage is considered on the lateral and bottom sides, as it was assumed that the earthquake does not cause detachment of the concrete in the top side of the beam. Fig. 2 illustrates the sections of columns and beams with damages D0/D1, D2 and D3. Damage in the structural elements is concentrated in the RC element ends (plastic hinge region), where the damage due to the seismic demand is usually located.

### 2.3. Fire action

In the initial step, thermal analyses were developed, considering the standard fire curve ISO 834 and parametric fire curves [30]. SAFIR calculates the temperature evolution as a function of time, and this data is used in the following step that corresponds to the mechanical analyses. Fig. 3 and Fig. 4 represent examples of temperature profiles of a column and beam, respectively, with damage D0/D1, D2 and D3 after one hour considering the fire curve ISO 834. Additionally, Fig. 5 and Fig. 6 represent examples of temperature profiles for a column and beam, respectively, with damage D0/D1 at 30, 60 and 90 min, considering a parametric fire curve.

It should be noticed that in Fig. 5 and Fig. 6, the temperature profiles at 60 and 90 min represent the cooling phase of the parametric fire curve. It is observed that the temperature begins to decrease and tends to be higher near the steel reinforcement due to the higher thermal conductivity of the steel reinforcement compared to concrete.

These temperature profiles, along with other similar ones, are then used in the subsequent step that corresponds to the mechanical analysis. Additional details regarding the characteristics of the parametric fire curves are presented in the following section.

**Table 1**
Parameters of the established distributions for the considered properties of the frames.

| Variables | Mean | CV (%) | A | B | Distribution |
|---|---|---|---|---|---|
| $H_1$ (m) | 3.2 | 10 | 2.5 | 5 | Lognormal |
| $H_{>1}$ (m) | 2.8 | 6 | 2.5 | 4 | Normal |
| $L_{beam}$ (m) | 4.4 | 16 | 2.5 | 6.5 | Lognormal |
| $f_{cm}$ (MPa) | 23.8 | 49 | 18 | 36 | Gamma |
| G (kN/m$^2$) | 8 | 12.5 | 6 | 10 | Normal |
| $P_l$ (%) | 1 | 40 | 0.3 | 3.5 | Lognormal |
| $f_{yk}$ (MPa) | 235/400/500 | - | - | - | - |
| c (mm) | 10/15/20/25 | - | - | - | - |

## 3. Parametric study

### 3.1. Introduction

Numerical models of a three-bay and two-floor plane frame were developed to evaluate the post-earthquake fire phenomenon. A schematic representation of the frame developed in these analyses is presented in Fig. 7. The frame has six compartments, C11, C12 and C13 on the lower floor, and compartments C21, C22 and C23 on the upper floor. Uniformly distributed loads were considered in the beams and vertical loads in the columns. The damage was always considered at the ends of the columns and beams, with a length equal to the section size of the respective elements (column or beam), and equal to the expected plastic hinge zone. For each configuration, damage D0/D1, D2 and D3 were considered [12].

This section encompasses several studies based on the described frame. The first study aimed to assess the influence of the location of the damage and two configurations were considered, namely one where the damage is located in the whole frame and a second configuration where the damage is considered only in the bottom floor. The second study explored the influence of the number of exposed sides in the lateral columns, and three configurations were considered, which were the lateral columns with one, three and four heated sides. The third study evaluated the influence of the fire location and four configurations with different locations of the fire were considered. Finally, a fourth study examined the influence of different parametric fire curves with and without active firefighting measures. Some of the frame configurations from the second and third studies were also included in the fourth study.

### 3.2. Properties and characteristics of the frames

To accurately develop numerical models representative of a building stock of RC buildings designed without seismic concerns, it is important to adequately ascertain the properties and characteristics of the buildings. The parameters required to define the numerical models were obtained from a report allowing the seismic safety evaluation of existing

**Table 2**
Concrete properties used in the numerical analyses.

| Concrete properties [23] | |
|---|---|
| Concrete model | Siliceous aggregates [23] |
| Specific mass of concrete | 2300 kg/m3 |
| Water content | 26 kg/m3 |
| Emissivity | 0,7 |
| Tensile strength | 0 |
| Poisson's ratio | 0,2 |

**Table 3**
Reinforcing steel properties used in the numerical analyses.

| Reinforcing steel properties [23,35] | |
|---|---|
| Steel model | Hot rolled. class B [23,35] |
| Modulus of elasticity | 210 GPa |
| Poisson's ratio | 0,3 |
| Emissivity | 0,7 |

RC buildings [31]. The parameters of the established probability distributions for the considered properties of the frames are presented in Table 1, where the variable $H_1$ corresponds to the height of the first floor, $H_{>1}$ is the height of the second floor, $L_{beam}$ is the length of the beams, $f_{cm}$ is the mean value of concrete compressive strength, G is the self-weight, $P_l$ is the percentage of longitudinal reinforcing steel, $f_{yk}$ is the characteristic yield strength of the reinforcing steel and c is the cover of the columns and beams. It also includes parameters A and B, which are the truncation values considered. The remaining parameters required for the numerical models, namely the properties of concrete and reinforcing steel, are presented in Table 2 and Table 3, respectively. The design of the frames followed the criteria presented in the Portuguese regulation for RC structures [32–34], which, during that particular period, did not require seismic considerations for these frames. The values of the cover are based on the indications in this regulation, resulting in the definition of four different values for the cover to represent various constructive arrangements. The thermal conductivity value is set in the middle, between the upper limit and lower limit provided by NP EN 1992–1-2 [23].

The design of each frame began with a random selection (not correlated) of a value from each variable presented in Table 1. In the case of the $f_{yk}$ and the cover, the presented values had an equal probability of being selected. Based on this procedure, 100 different frames were developed, where the properties presented in Table 2 and Table 3 are constant in all frames. In subsequent studies, different considerations regarding the location and type of seismic damage and the location and type of the fire were examined for these 100 frames.

### 3.3. Influence of the damage location

To investigate the influence of the type and location of damage on the time until the collapse of the frames, two different configurations were considered. First, the damage was considered on both floors of the frame, and secondly, another configuration involved damage only on the lower floor. In this case, the fire impacted only the compartments on the lower floor (compartments C11, C12 and C13). In the columns, fire was considered on all sides, while in the beams, fire was considered on three sides. For each configuration, damage D0/D1, D2 and D3 were considered. The frame configurations developed and analysed in this section are presented in Fig. 8.

After developing 100 frames for each type of damage (D0/D1, D2 and D3) and for each configuration (damage on both floors and damage on the lower floor), it is possible to compare and analyse the results obtained through the discrete data and the respective adjusted distribution. The percentage of exceedance of the time until the collapse of the frames is presented in Fig. 9, and the mean and standard deviation are presented in Table 4. The two frame configurations with damage D0/

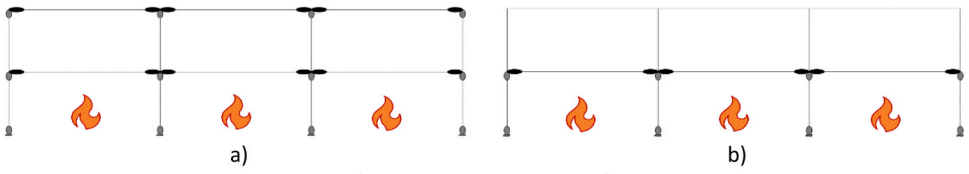


**Fig. 8.** Frame configurations; a) damage in both floors, b) damage only in the bottom floor.

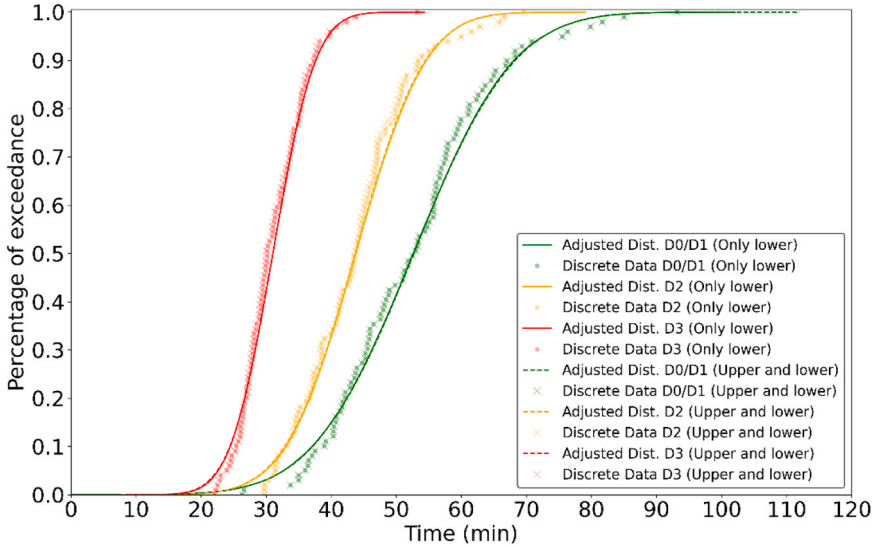


**Fig. 9.** Percentage of exceedance of the time until collapse of the frames with different damage locations, for damage D0/D1, D2 and D3.

**Table 4**
Mean and Standard Deviation of the time until collapse of the frames with different damage locations, for damage D0/D1, D2 and D3.

| Damage location | Damage | Mean | Standard Deviation |
|---|---|---|---|
| Upper and lower floors | D0/D1 | 52.71 | 12.18 |
| | D2 | 43.69 | 8.42 |
| | D3 | 31.08 | 5.12 |
| | D0/D1 | 52.71 | 12.18 |
| Only lower floor | D2 | 43.73 | 8.45 |
| | D3 | 31.15 | 5.15 |

D1 correspond to the same numerical model, therefore the results are duplicated in Fig. 9 and in Table 4. By comparing the results of both configurations for the damage location, it is observed that the results are similar. This suggests that considering damage in the same location where the fire is occurring may be a reasonable approach, rather than considering more detailed or complex damage configurations in the frames. From the frames with damage D0/D1, the highest time until collapse observed is 93 min, and the lowest time until collapse is 26 min. For the frames with damage D3, the highest time until collapse observed is 53 min, and the lowest time until collapse is 22 min. The higher standard deviation in the results indicates a higher variability of the results of the frames with damage D0/D1 compared to the frames with damage D2, and of these when compared with the frames with damage D3. This aspect can be related to the cover of the beams and columns. In the frames with damage D3, the collapse is expected to be governed by the failure in the extremities of the columns and/or beams, where the damage is located, and the steel reinforcement is exposed to fire. In the case of the frames with damage D0/D1, there is a variability in the cover in these zones, which can explain the higher variability in the results of the frames with damage D0/D1. These results clearly demonstrate the impact of the earthquake damage on the fire resistance of the RC frames.

### 3.4. *Influence of different sides exposed to fire in the lateral columns*

In this section, the influence of exposing different sides of the lateral columns to fire on the time until collapse is analysed. The frame configurations are presented in Fig. 10. Three different configurations were developed, one where the lateral columns were exposed on one side, another where the lateral columns were exposed on three sides, and the last one where they were heated on all sides (which is one of the configurations considered in Section 3.3). The interior columns were exposed on all sides, and the beams on three sides.

The percentage of exceedance of the time until the collapse of the developed frames is presented in Fig. 11, and the mean and standard deviation are presented in Table 5. When comparing the results between the three configurations, it is observed a significant difference, especially in the frames with damage D0/D1. These differences highlight the importance of a careful definition of the sides exposed to fire in the elements. Similar to the previous section, there is a higher variability in the results of frames with damage D0/D1 compared to frames with damage D2, and of these when compared with the frames with damage D3. The configuration where the lateral columns are heated on three sides seems to be the configuration that best represents what happens in a real fire scenario, considering that the fire is inside the compartment and not outside. It can be assumed that walls may not provide sufficient protection against fire in a post-earthquake scenario due to earthquake damage. This aspect makes the configuration where the lateral columns are heated only on one side unlikely to occur.

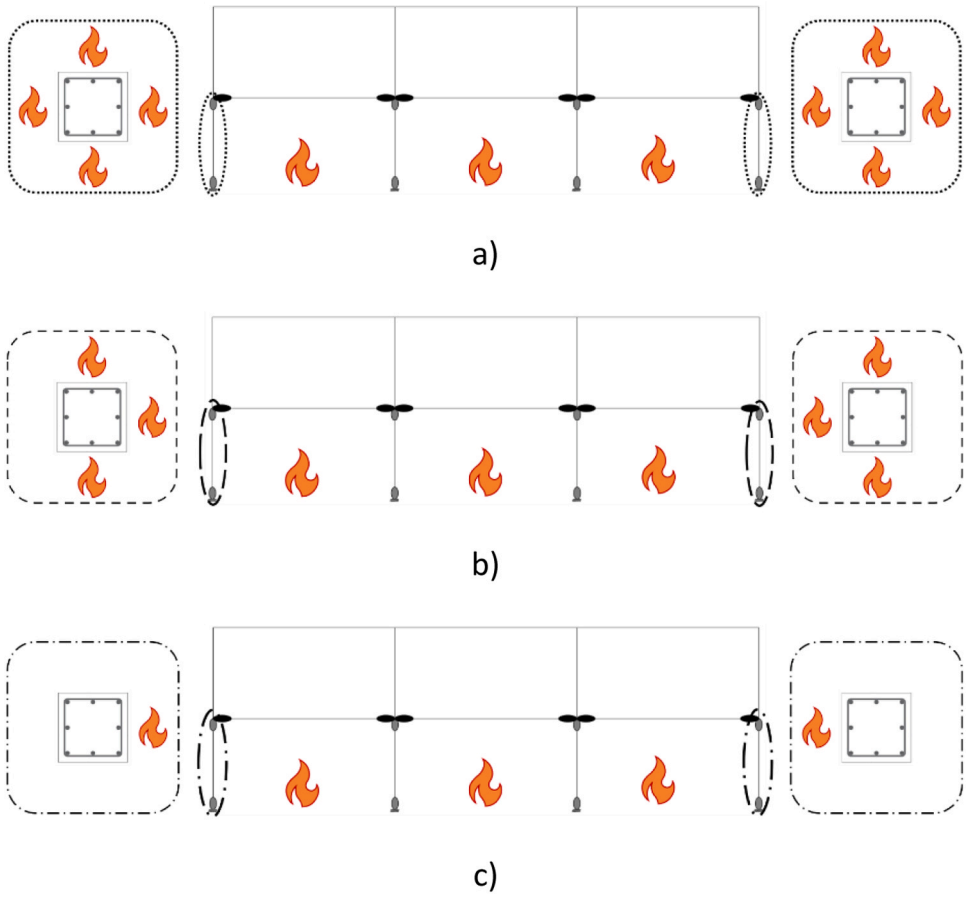


**Fig. 10.** Frame configuration with the location of damage and fire: a) four sides exposed to fire in the lateral columns, b) three sides exposed to fire in the lateral columns and c) one fire frontier in the lateral columns.

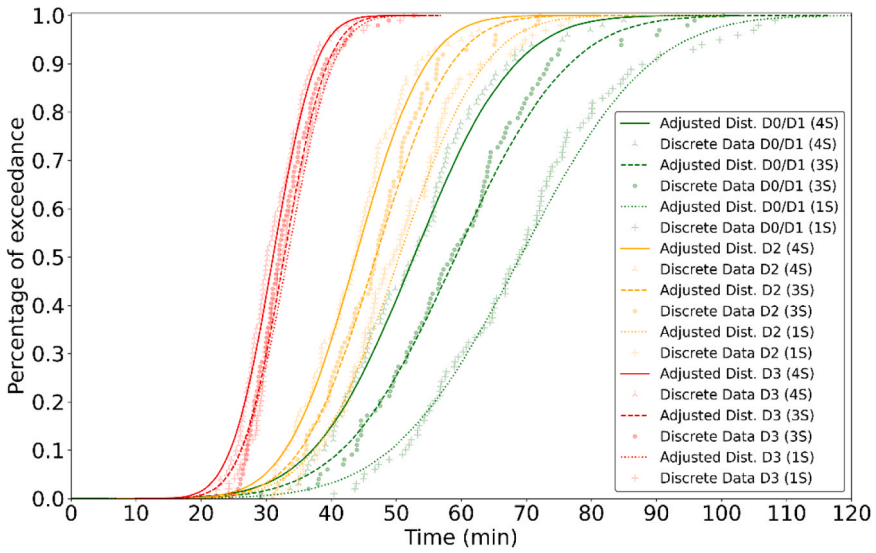


**Fig. 11.** Percentage of exceedance of the time until collapse of the frames with different sides exposed to fire in the lateral columns (4 S, 3 S, 1 S).

**Table 5**
Mean and Standard Deviation of the time until collapse of the frames with different sides exposed to fire in the lateral columns, for damage D0/D1, D2 and D3.

| Sides exposed to fire in lateral column | Damage | Mean | Standard Deviation |
|---|---|---|---|
| | *D0/D1* | *52.71* | *12.18* |
| *4 S* | *D2* | *43.73* | *8.45* |
| | *D3* | *31.15* | *5.15* |
| | D0/D1 | 59.13 | 13.68 |
| 3 S | D2 | 46.91 | 9.11 |
| | D3 | 32.86 | 5.23 |
| | D0/D1 | 69.04 | 15.70 |
| 1 S | D2 | 50.49 | 10.36 |
| | D3 | 33.28 | 5.52 |

### 3.5. Influence of the Fire Location

In this section, it is analysed the influence of different fire locations on the time until the collapse of the frames. The frame configurations are presented in Fig. 12. Four different configurations were considered: the first, where the fire was considered in all compartments of the lower floor (compartment C11, C12 and C13); the second, where the fire was considered in compartment C11; the third, where the fire was considered in compartment C12; and finally, the fourth, where the fire was considered in compartments C11 and C12. It is worth mentioning that the first configuration in this section is the same as the one presented in Section 3.4 with three sides exposed to fire in the lateral columns. In these configurations, if the fire is in the lateral compartments (C11 and/or C13), the lateral columns were always defined with three sides exposed to fire. If both adjacent compartments of an interior column were subjected to fire, then the interior column had four heated sides, otherwise, the interior column had three exposed sides. The beams were exposed on three sides.

The percentage of exceedance of the time until the collapse of the developed frames is presented from Fig. 13 to Fig. 15, and the mean and standard deviation are presented in Table 6. In Fig. 16, the mean of the time until the collapse of the frames with different fire locations, for damage D0/D1, D2 and D3, is represented.

The comparison between the results of the different configurations indicates that considering fire in different compartments can lead to significantly different results. Applying fire in all compartments of the first floor (C11, C12 and C13) can be the more suitable approach since it is the more severe configuration when considering damage D0/D1 and D2 and with relatively similar results for damage D3. These results show that the type of damage in the compartments where the fire is applied can affect the definition of the worst fire scenario, where having the whole floor on fire does not necessarily translate into having the lower times until collapse. The significant difference between the results of the configurations C11 and C12 can be highlighted by the fact that there are two different columns in the frame, the interior columns, and the lateral columns, where the lateral columns have a lower cross-section when compared with the interior columns. This aspect can be the main reason for the lower times until collapse of the configuration C11 when compared with configuration C12. The observed differences highlight the impact of the fire location on the time until the collapse of the

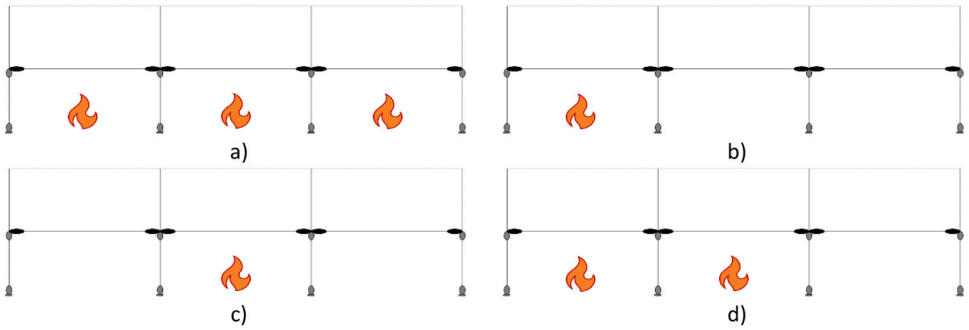


**Fig. 12.** Frame configurations; a) fire in all the compartments of the bottom floor (C11 C12 C13), b) fire in the left compartment of the bottom floor (C11), c) fire in the middle compartment of the bottom floor (C12) and d) fire in the left and middle compartments of the bottom floor (C11 C12).

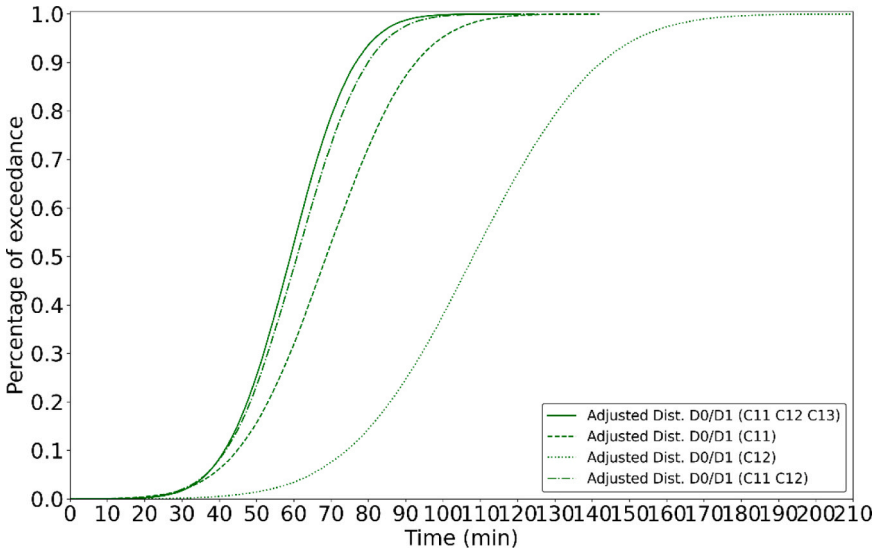


**Fig. 13.** Percentage of exceedance of the time until collapse of the frames with damage D0/D1 and with different fire locations.

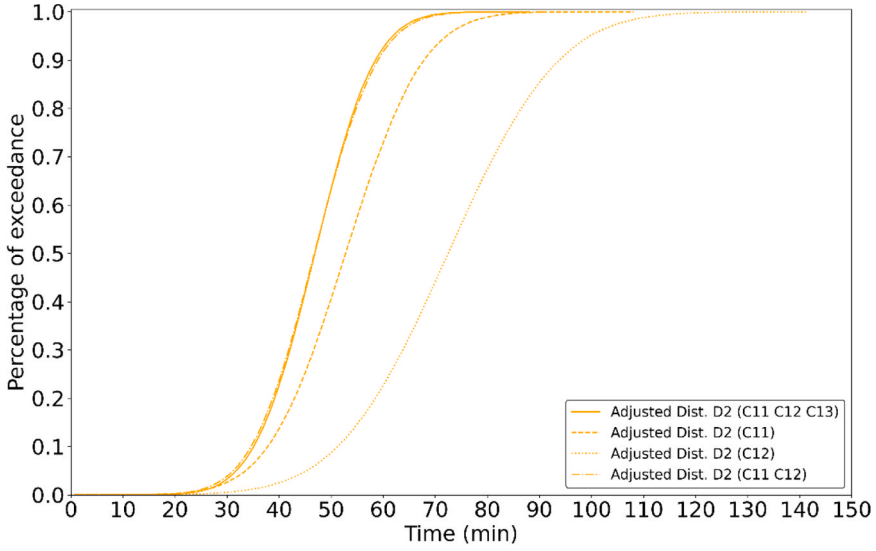


**Fig. 14.** Percentage of exceedance of the time until collapse of the frames with damage D2 and with different fire locations.

frames, demonstrating the importance of their accurate definition.

### 3.6. Impact of the fire curves

To compare the differences in considering the parametric fire curves versus the ISO 834 fire curve on the frames, parametric fire curves were developed for each of the 100 RC frames, with and without considering active firefighting measures [36]. In a post-earthquake scenario, it is plausible to expect malfunctioning of the passive and active fire protection systems and delays in the firefighter's response. These can be represented by the parametric fire curves where no active firefighting measures are considered. This scenario can be then compared with a scenario where the active firefighting measures are considered, representing a generic situation where fire can occur at any given time. The curves represent compartment fires in dwellings with a quadrangular shape, two openings in the walls, one door (0.8 × 2.0 m) and one window (0.4 L × 0.4 H). The dimension of the window corresponds to 40% of the size of the compartment walls. It was observed in the literature that this is a common type of configuration of the openings in masonry infill walls [37]. For this fire compartment, the material properties are given in Table 7, and the active firefighting measures are presented in Table 8 and in Table 9. All the curves developed are plotted in Fig. 17.

#### 3.6.1. Damage and fire on the lower floor

In this section, the influence of different fire curves (parametric and ISO 834 fire curves) on the time until the collapse of the RC frames is analysed for the frame configuration presented in Fig. 12 a), consisting of damage and fire on the lower floor. For the sake of comparison, the results of the frames presented earlier are replicated herein.

The results of the frames when considering the parametric fire curves with no active firefighting measures are compared to the results of the frames when considering the fire curve ISO 834. The percentage of exceedance of the time until the collapse of the developed frames is presented in Fig. 18, and the mean and standard deviation are presented in Table 10. The consideration of parametric fire curves with no active firefighting measures leads to lower times until collapse when compared with the use of the fire curve ISO 834. It is observed, approximately, a 10-minute reduction in the time until the collapse of the frames where the parametric curves with no active firefighting measures are used when compared with using the fire curve ISO 834. Damage in the passive

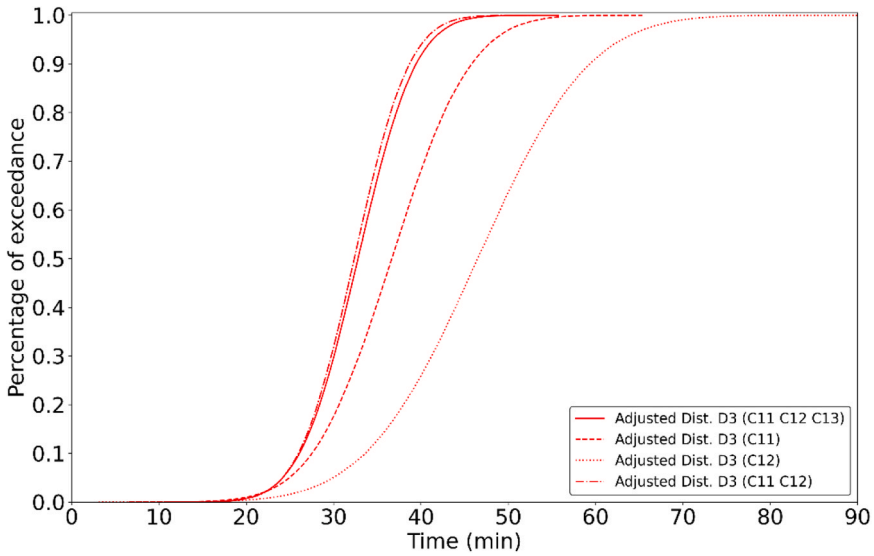


**Fig. 15.** Percentage of exceedance of the time until collapse of the frames with damage D3 and with different fire locations.

**Table 6**
Mean and Standard Deviation of the time until collapse of the frames with different fire locations, for damage D0/D1, D2 and D3.

| Fire Location | Damage | Mean | Standard Deviation |
|---|---|---|---|
| | *D0/D1* | *59.13* | *13.68* |
| *C11 C12 C13* | *D2* | *46.91* | *9.11* |
| | *D3* | *32.86* | *5.23* |
| | D0/D1 | 68.80 | 18.69 |
| C11 | D2 | 52.79 | 11.73 |
| | D3 | 36.67 | 7.14 |
| | D0/D1 | 108.32 | 26.59 |
| C12 | D2 | 72.48 | 16.67 |
| | D3 | 46.44 | 10.02 |
| | D0/D1 | 60.91 | 14.93 |
| C11 C12 | D2 | 46.82 | 9.49 |
| | D3 | 32.32 | 4.98 |

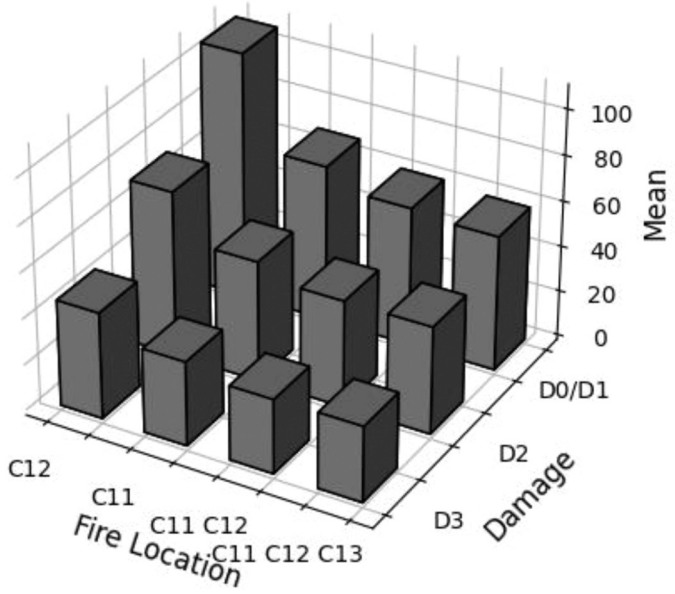


**Fig. 16.** Mean of the time until collapse of the frames with different fire locations, for damage D0/D1, D2 and D3 considering the fire curve ISO 834.

**Table 7**
Properties of the materials in the fire compartments.

| Material | Properties | | | |
|---|---|---|---|---|
| | Thickness (cm) | Unit mass (kg/m$^3$) | Conductivity (W/mK) | Specific Heat (J/kgK) |
| Normal weight concrete | 20 | 2300 | 1.6 | 1000 |
| Brick 1 | 15 | 625 | 0.36 | 840 |
| Brick 2 | 11 | 654 | 0.38 | 840 |

and active fire protection systems and delays in the response of the firefighters is a plausible scenario after an earthquake, and this aspect can be represented by using parametric curves with no active fire-fighting measures. When analysing the fire resistance of a structure after an earthquake, perhaps the best approach would be to use the parametric fire curves instead of the fire curve ISO 834, to favour a more conservative approach.

For the parametric fire curves with active firefighting measures, Table 11 presents the number of frames that collapsed and that did not collapse. For damage D0/D1, there is collapse of 3% of the frames, and for damage D3, there is collapse of 27% of the frames, which shows the impact of the damage on the fire resistance of the frames. It is observed that there is a strong correlation between the number of frames that did not collapse and the type of damage, namely it is observed that the number of collapses increases with the severity of the damage. Since there are a high number of structures that have shown no collapse, the results were not analysed and compared in terms of the adjusted distributions presented in Fig. 18. An interesting phenomenon was observed in the frames where it was considered the parametric fire curves with active firefighting measures, which was the collapse of some of those frames after the maximum temperature peak on the respective parametric fire curve. The temperature in the RC sections continues to increase after reaching the maximum temperature of the parametric fire curve, and this aspect sometimes can lead to the collapse of structures in the cooling phase. For the frames with damage D2 almost all the frames collapsed after the time of the maximum temperature.

These results emphasize the importance of knowing that frames can collapse even if the fire is in a cooling phase. It is especially important because this phase may correspond to the aftermath of a fire and there is a possibility of firefighters being inside the buildings. This phenomenon, for the configurations considered in this section, is not observed when it is considered the parametric fire curves without active firefighting

**Table 8**
Factors of the Active Fire Fighting Measures (no measures considered) [36].

| Automatic Fire Suppression | | Automatic Fire Detection | | Manual Fire Suppression | | | | |
|---|---|---|---|---|---|---|---|---|
| Automatic Water Extinguishment System | Independent Water Supplies | Automatic Fire Detection and Alarm | Automatic Alarm Transmission to Fire Brigade | Work Fire Brigade | Off Site Brigade | Safe Access Routes | Fire Fighting Devices | Smoke Exhaust System |
| 1.0 | 1.0 | 1.0 | 1.0 | 1.0 | 1.0 | 1.5 | 1.5 | 1.5 |

**Table 9**
Factors of the Active Fire Fighting Measures (measures considered) [36].

| Automatic Fire Suppression | | Automatic Fire Detection | | Manual Fire Suppression | | | | |
|---|---|---|---|---|---|---|---|---|
| Automatic Water Extinguishment System | Independent Water Supplies | Automatic Fire Detection and Alarm | Automatic Alarm Transmission to Fire Brigade | Work Fire Brigade | Off Site Brigade | Safe Access Routes | Fire Fighting Devices | Smoke Exhaust System |
| 0.61 | 1.0 | 0.73 | 1.0 | 1.0 | 0.78 | 1.0 | 1.0 | 1.5 |

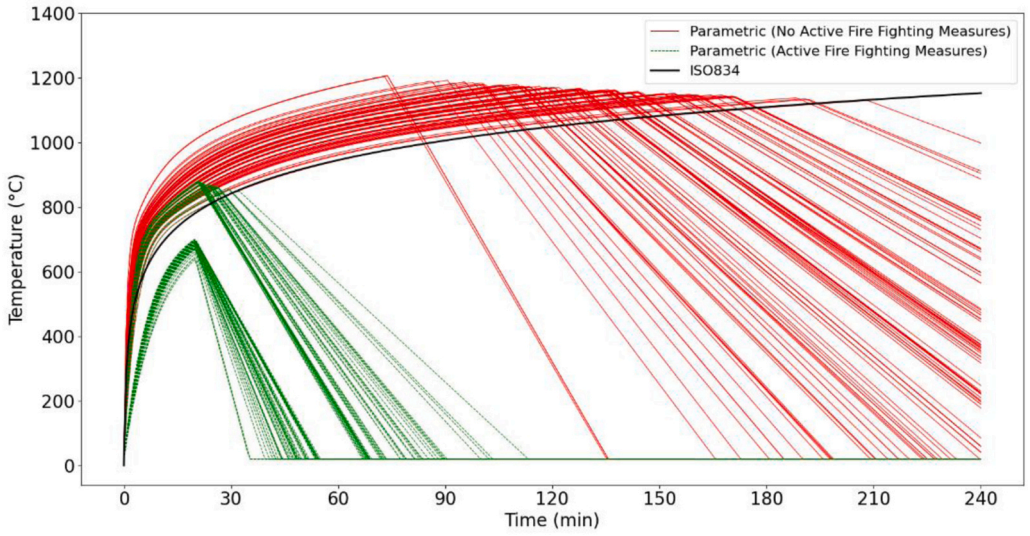


**Fig. 17.** Parametric fire curves considered in the frames.

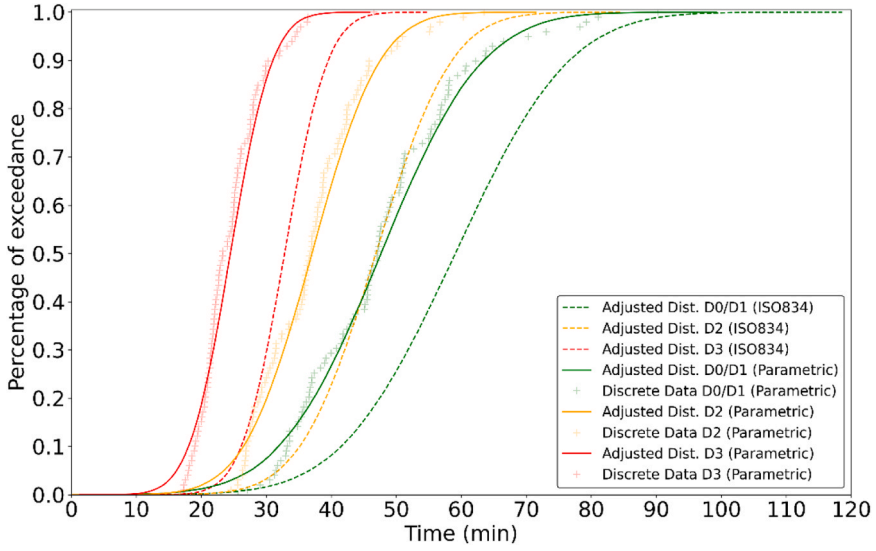


**Fig. 18.** Percentage of exceedance of the time until collapse of the frames considering the fire curve ISO 834 and parametric fire curves with no active firefighting measures, for damage D0/D1, D2 and D3.

**Table 10**
Mean and Standard Deviation of the time until collapse of frames considering the fire curve ISO 834 and parametric fire curves with no active firefighting measures, for damage D0/D1, D2 and D3.

| Model | Damage | Mean | Standard Deviation |
|---|---|---|---|
| *ISO 834* | *D0/D1* | *59.13* | *13.68* |
| | *D2* | *46.91* | *9.11* |
| | *D3* | *32.86* | *5.23* |
| Parametric without active firefighting measures | D0/D1 | 47.75 | 12.29 |
| | D2 | 36.99 | 8.19 |
| | D3 | 24.51 | 5.06 |

**Table 11**
Number of frames that collapsed and that did not collapse when considering parametric fire curves with active firefighting measures, for damage D0/D1, D2 and D3.

| Model | Damage | No Collapse | Collapse | Collapse (cooling phase) |
|---|---|---|---|---|
| Parametric with active firefighting measures | D0/D1 | 97 | 3 | 2 |
| | D2 | 95 | 5 | 4 |
| | D3 | 73 | 27 | 15 |

measures.

### 3.6.2. *Influence of the location of the fire*

In this section, the influence of considering the location and different fire curves on the time until collapse of the frames is analysed. The frame configurations considered herein are those presented in Fig. 12, and previous results are replicated in this section for the sake of comparison.

The percentage of exceedance of the time until the collapse of the developed frames is presented from Fig. 19 to Fig. 21, and the mean and standard deviation are presented in Table 12. In Fig. 22, the mean of the time until collapse of the frames with different fire locations, for damage D0/D1, D2 and D3 is represented.

The consideration of parametric fire curves with no active firefighting measures leads to lower times until collapse when compared with the fire curve ISO 834. As in the previous section, in most of the cases, it is observed at least a 10-minute reduction in the time until collapse of the frames when using the parametric curves with no active firefighting measures versus using the ISO 834 fire curve. For the scenario with damage D0/D1 and fire in the middle compartment (C12), there were three frames that did not collapse therefore these frames were disregarded. For that same scenario, it was observed that three frames collapsed after the time of the maximum temperature of the respective parametric fire curves with no active firefighting measures. In those three frames, the collapse occurred 4.72, 5.23 and 4.31 min after the time of the maximum temperature. Also, for the scenario with damage D0/D1 where the fire is only in the left compartment (C11) there was one frame that collapsed 7.23 min after the time of the maximum temperature of the parametric fire curve. The number of frames that did and did not collapse when considering parametric fire curves with active firefighting measures are presented in Table 13. Once again, it is observed the impact of the damage on the fire resistance of the frames. There is a considerable number of frames that collapsed after the time of the maximum temperature of the parametric fire curve is reached. This type of collapse mainly happens when considering parametric fire curves with active firefighting measures, which can be explained by the fact that in these parametric curves, the cooling phase starts much sooner than in the parametric fire curves without active firefighting measures.

## 4. Conclusions

In this study, 100 RC frames representative of a building stock designed without seismic concerns were developed to analyse the impact of earthquake damage, the number of sides exposed to fire, fire locations, and fire curves on the fire resistance of the RC frames in a post-earthquake scenario.

Generally, the results show that frames with severe damage (damage D3) have significantly lower fire resistance when compared to undamaged frames (damage D0/D1). Furthermore, based on all the developed studies, a reduction of 17–35% in the mean fire resistance of the frames with damage D2 was observed when compared to the frames with damage D0/D1, and a reduction of 41–59% in the mean fire resistance of the frames with damage D3 when compared to the frames with damage D0/D1. This aspect indicates the high impact that the type of damage can have on the time until the collapse of the frames.

Additionally, a higher variability in the results of the frames with damage D0/D1 compared to the frames with damage D2, and of these when compared with the frames with damage D3, was observed. This aspect can be related to the cover of the RC sections, where the sections with damage D0/D1 have an intact cover, while the sections with damage D3 are without cover.

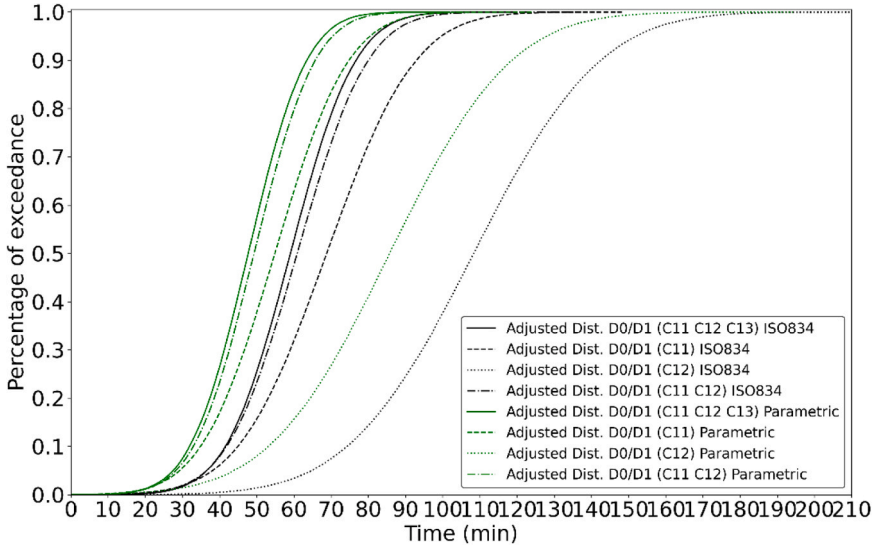


**Fig. 19.** Percentage of exceedance of the time until collapse of the frames with damage D0/D1, with different fire locations considering the fire curve ISO 834 and parametric fire curves with no active firefighting measures.

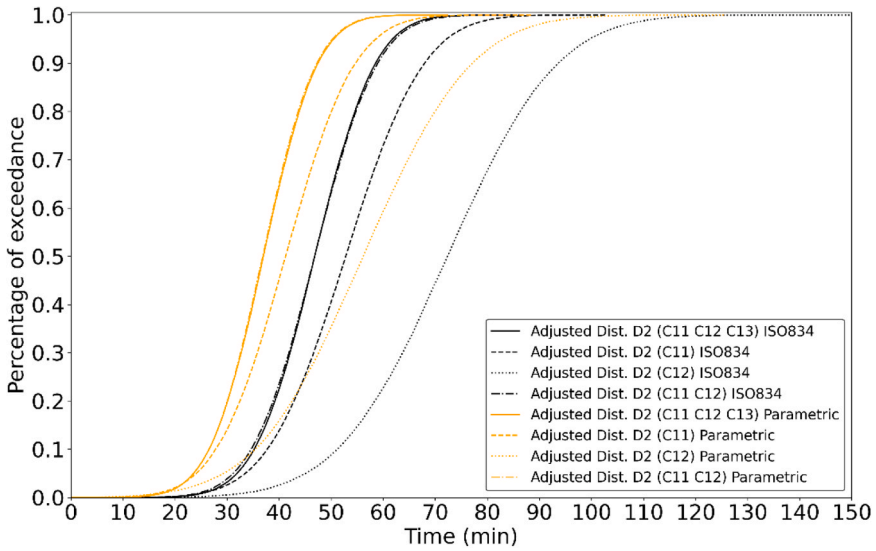


**Fig. 20.** Percentage of exceedance of the time until collapse of the frames with damage D2, with different fire locations considering the fire curve ISO 834 and parametric fire curves with no active firefighting measures.

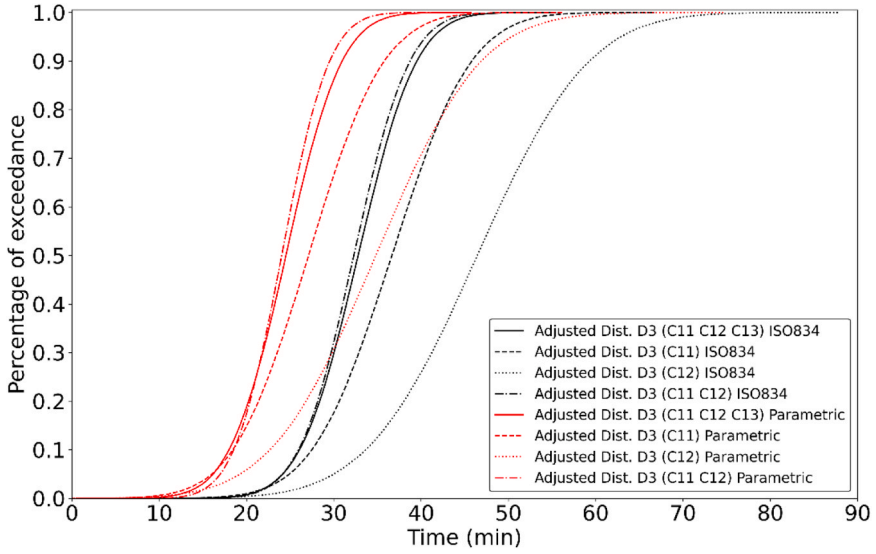


**Fig. 21.** Percentage of exceedance of the time until collapse of the frames with damage D3, with different fire locations considering the fire curve ISO 834 and parametric fire curves with no active firefighting measures.

**Table 12**
Mean and Standard Deviation of the time until collapse of frame with different fire locations considering parametric fire curves with no active firefighting measures, for damage D0/D1, D2 and D3.

| Model | Damage | Mean | Standard Deviation |
|---|---|---|---|
| | *D0/D1* | *47.75* | *12.29* |
| *C11 C12 C13* | *D2* | *36.99* | *8.19* |
| | *D3* | *24.51* | *5.06* |
| | D0/D1 | 54.83 | 15.63 |
| C11 | D2 | 41.29 | 10.43 |
| | D3 | 27.12 | 6.76 |
| | D0/D1 | 85.84 | 25.55 |
| C12 | D2 | 56.17 | 16.31 |
| | D3 | 34.83 | 9.46 |
| | D0/D1 | 49.23 | 12.86 |
| C11 C12 | D2 | 36.83 | 8.07 |
| | D3 | 24.03 | 4.28 |

The studies showed that when there is a fire on the bottom floor, there is a minimal difference in the times until the collapse between the frames that have damage on the bottom floor and the frames that have damage on both floors. This aspect indicates that a complex characterization of the damage may not be necessary.

Regarding different exposed sides in the lateral columns, significantly different results were observed, especially in frames with damage D0/D1 and even D2. For the influence of the location of the fire, it was observed that having fires in different compartments can lead to a significant difference in the results and that the damage in the compartments where the fire is applied can impact the definition of the worst fire scenario. In particular, it was observed that having more compartments subjected to fire does not necessarily signify having lower times until collapse.

The comparison between different fire curves indicates that, for post-earthquake fire scenarios, using parametric fire curves without active firefighting measures leads to lower time until the collapse of the frames compared to using the ISO 834 fire curve, making it a more conservative

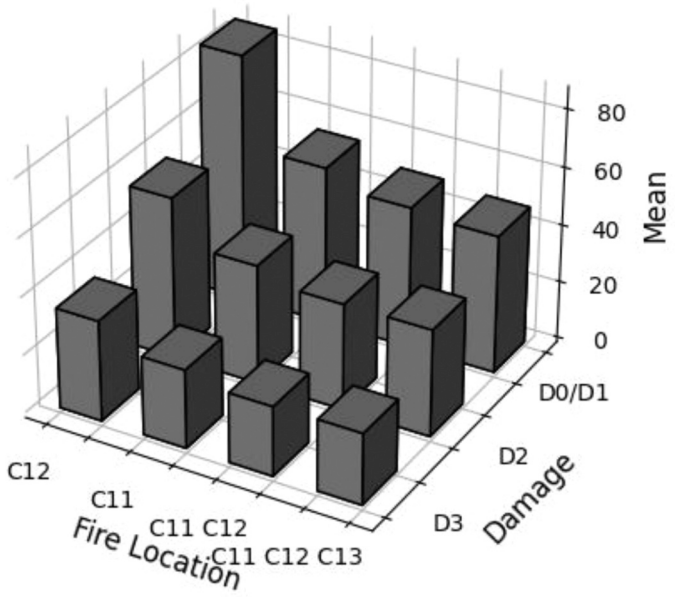


**Fig. 22.** Mean of the time until collapse of the frames with different fire locations, for damage D0/D1, D2 and D3 considering the parametric fire curves with no active firefighting measures.

**Table 13**
Number of frames that collapsed and that did not collapse when considering the parametric fire curves with active firefighting measures, for different fire locations, for damage D0/D1, D2 and D3.

| Model | Damage | No collapsed | Collapse | Collapse (cooling phase) |
|---|---|---|---|---|
| *C11 C12 C13* | *D0/D1* | *97* | *3* | *2* |
| | *D2* | *95* | *5* | *4* |
| | *D3* | *73* | *27* | *15* |
| C11 | D0/D1 | 100 | 0 | 0 |
| | D2 | 98 | 2 | 0 |
| | D3 | 84 | 16 | 10 |
| C12 | D0/D1 | 100 | 0 | 0 |
| | D2 | 100 | 0 | 0 |
| | D3 | 100 | 0 | 0 |
| C11 C12 | D0/D1 | 97 | 3 | 2 |
| | D2 | 95 | 5 | 4 |
| | D3 | 70 | 30 | 11 |

approach. For the parametric fire curves with active firefighting measures, a considerable number of frames did not collapse, indicating the high importance of adopting firefighting measures such as automatic fire detection and alarm, offsite brigade, safe access routes, and firefighting devices for preventing the collapse of structures. Another important observation drawn from these results is that some frames collapsed after the peak temperature of the parametric fire curve was reached, meaning that structural failure occurs during the cooling phase of the fire. This subject will be addressed in more detail in future studies.

Finally, several other critical factors that could affect the structure's integrity due to an earthquake event were not considered in this study. However, the present study aimed to improve the comprehension of the post-earthquake fire in RC frames, demonstrating that to improve the fire resistance and even prevent the collapse of the structures, limiting the earthquake structural damage and avoiding damage in the active and passive fire protection systems in a post-earthquake scenario are vital strategies. Nevertheless, it is important to develop more extensive and in-depth studies to draw more meaningful conclusions that could help develop guidelines and prescriptive measures to reduce the risks associated with post-earthquake fires.

## Author statement

**H. Vitorino:** Conceptualization, Formal analysis, Investigation, Writing - Original Draft. **P. Vila Real:** Conceptualization, Methodology, Investigation, Writing - Review & Editing, Supervision. **C. Couto:** Conceptualization, Methodology, Investigation, Writing - Review & Editing, Supervision. **H. Rodrigues:** Conceptualization, Methodology, Investigation, Writing - Review & Editing, Supervision.

## CRediT authorship contribution statement

**Vitorino Hugo:** Writing – original draft, Methodology, Investigation, Conceptualization. **Couto Carlos:** Writing – review & editing, Supervision, Methodology, Investigation, Conceptualization. **Vila Real Paulo:** Writing – review & editing, Supervision, Methodology, Investigation, Formal analysis, Conceptualization. **Rodrigues Hugo:** Writing – review & editing, Supervision, Methodology, Investigation, Conceptualization.

## Declaration of Competing Interest

The authors whose names are listed in the paper certify that they have no Conflicts of Interest or involvement in any organization or entity with any financial interest (such as honoraria; educational grants; participation in speakers' bureaus; membership, employment, consultancies, stock ownership, or other equity interest; and expert testimony or patent-licensing arrangements), or non-financial interest (such as personal or professional relationships, affiliations, knowledge or beliefs) in the subject matter or materials discussed in this manuscript.

Moreover, the authors declare that all named authors in the manuscript are aware of the submission and have agreed for the paper to be submitted to Engineering Structures.

## Data availability

Data will be made available on request.

## Acknowledgements

This work was supported by the Foundation for Science and Technology (FCT) – Aveiro Research Centre for Risks and Sustainability in Construction (RISCO), University of Aveiro, Portugal [FCT/UIDB/ECI/04450/2020]. The first author acknowledged to FCT – Foundation for Science and Technology namely through the PhD grant with reference SFRH/BD/148582/2019. This work was also financially supported by Project 2022.02100. PTDC – "Post Earthquake Fire Risk AssessMEnt at Urban Scale" funded through FCT/MCTES.

## References

[1] R. Botting and A. Buchanan, "The Impact of Post-Earthquake Fire on the Urban Environment," 1998.
[2] Khorasani NE, Garlock MEM. Overview of fire following earthquake: historical events and community responses. Int J Disaster Resil Built Environ 2017;vol. 8(2): 158–74. https://doi.org/10.1108/IJDRBE-02-2015-0005.
[3] Baker GB, Collier PCR, Abu AK, Houston BJ. Post-earthquake structural design for fire – a New Zealand perspective. 7th Int Conf Struct Fire 2012:1–10.
[4] C. Scawthorn, "The ShakeOut Scenario - Fire Following Earthquake," 2008. doi: 10.3801/iafss.fss.1–971.
[5] Himoto K. Comparative analysis of post-earthquake fires in Japan from 1995 to 2017. Fire Technol 2019;vol. 55(3):935–61. https://doi.org/10.1007/s10694-018-00813-5.
[6] Sekizawa A, Sasaki K. Study on fires following the 2011 great East-Japan earthquake based on the questionnaire survey to fire departments in affected areas. Fire Saf Sci 2014;vol. 11:691–703. https://doi.org/10.3801/IAFSS.FSS.11-691.
[7] Yu J, et al. A survey of impact on industrial parks caused by the 2011 Great East Japan earthquake and tsunami. J Loss Prev Process Ind 2017;vol. 50:317–24. https://doi.org/10.1016/j.jlp.2017.01.020.
[8] Behnam B, Ronagh H. Performance of reinforced concrete structures subjected to Fire following earthquake. Eur J Environ Civ Eng 2013;vol. 17(4):270–92. https://doi.org/10.1080/19648189.2013.783882.

[9] Behnam B, Ronagh HR. Post-earthquake fire resistance of CFRP strengthened reinforced concrete structures. Struct Des Tall Spec Build 2011;vol. 23(March 2013):814–32. https://doi.org/10.1002/tal.
[10] Behnam B, Ronagh HR, Baji H. Methodology for investigating the behavior of reinforced concrete structures subjected to post earthquake fire. Adv Concr Constr 2013;vol. 1(1):29–44. https://doi.org/10.12989/acc.2013.1.1.029.
[11] Ronagh HR, Behnam B. Investigating the effect of prior damage on the post-earthquake fire resistance of reinforced concrete portal frames. Int J Concr Struct Mater 2012;vol. 6(4):209–20. https://doi.org/10.1007/s40069-012-0025-9.
[12] Behnam B, Lim PJ, Ronagh HR. Plastic hinge relocation in reinforced concrete frames as a method of improving post-earthquake fire resistance. Structures 2015; vol. 2:21–31. https://doi.org/10.1016/j.istruc.2014.12.003.
[13] Vitorino H, Rodrigues H, Couto C. Evaluation of post-earthquake fire capacity of a reinforced concrete one bay plane frame under ISO fire exposure. Structures 2020; vol. 23(November 2019):602–11. https://doi.org/10.1016/j.istruc.2019.12.009.
[14] Vitorino H, Rodrigues H, Couto C. Evaluation of post-earthquake fire capacity of reinforced concrete elements. Soil Dyn Earthq Eng 2020;vol. 128(May 2019): 105900. https://doi.org/10.1016/j.soildyn.2019.105900.
[15] Vitorino H, Real PVila, Couto C, Rodrigues H. Post-earthquake fire assessment of reinforced concrete frame structures. Struct Eng Int 2022;(May). https://doi.org/10.1080/10168664.2022.2062084.
[16] Wu B, Liu F, Xiong W. Fire behaviours of concrete columns with prior seismic damage. Mag Concr Res 2017;vol. 69(7):365–78. https://doi.org/10.1680/jmacr.15.00497.
[17] Kamath P, et al. Full-scale fire test on an earthquake-damaged reinforced concrete frame. Fire Saf J 2015;vol. 73:1–19. https://doi.org/10.1016/j.firesaf.2015.02.013.
[18] Shah AH, Sharma UK, Bhargava P. Outcomes of a major research on full scale testing of RC frames in post earthquake fire. Constr Build Mater 2017;vol. 155: 1224–41. https://doi.org/10.1016/j.conbuildmat.2017.07.100.
[19] Shah AH, Sharma UK, Kamath P, Bhargava P, Reddy GR, Singh T. Fire performance of earthquake-damaged reinforced-concrete structures. Mater Struct/Mater Et Constr 2016;vol. 49(7):2971–89. https://doi.org/10.1617/s11527-015-0699-y.
[20] Shah AH, Sharma UK, Kamath P, Bhargava P, Reddy GR, Singh T. Effect of ductile detailing on the performance of a reinforced concrete building frame subjected to earthquake and fire. J Perform Constr Facil 2016;vol. 30(5):1–17. https://doi.org/10.1061/(ASCE)CF.1943-5509.0000881.
[21] D.C. Nwosu V.R. Kodur J. Franssen Use Man SAFIR: A Comput Program Anal Struct Elev Temp Cond, no January. 1999 doi: 10.4224/20331287.
[22] Franssen JM. 2005 SAFIR. A thermal/structural program for modelling structures under fire. Eng J 2005;vol. 42(3):143–58 [Online]. Available: http://orbi.ulg.ac.be/bitstream/2268/2928/1/2005 SAFIR. A thermal-structural program for modelling structures under fire - EJ.pdf.
[23] "Eurocode 2: Design of concrete structures - Part 1–2: General rules - Structural fire design," no. 2004, p. 99, 2011.
[24] Franssen JM, Gernay T. Modeling structures in fire with SAFIR®: theoretical background and capabilities. J Struct Fire Eng 2017;vol. 8(3):300–23. https://doi.org/10.1108/JSFE-07-2016-0010.
[25] Franssen JM. Failure temperature of a system comprising a restrained column submitted to fire. Fire Saf J 2000;vol. 34(2):191–207. https://doi.org/10.1016/S0379-7112(99)00047-8.
[26] Behnam B, Ronagh HR, Lim PJ. Numerical evaluation of the post-earthquake fire resistance of CFRP-strengthened reinforced concrete joints based on experimental observations. Eur J Environ Civ Eng 2016;vol. 20(2):142–60. https://doi.org/10.1080/19648189.2015.1018448.
[27] Ervine A, Gillie M, Stratford TJ, Pankaj P. Thermal Propagation through Tensile Cracks in Reinforced Concrete. J Mater Civ Eng 2012;(May):516–22. https://doi.org/10.1061/(ASCE)MT.1943-5533.0000417.
[28] Wu B, Xiong W, Wen B. Thermal fields of cracked concrete members in fire. Fire Saf J 2014;vol. 66:15–24. https://doi.org/10.1016/j.firesaf.2014.04.003.
[29] FEMA, "Prestandard and Commentary for the Seismic Rehabilitation of Buildings," 2000.
[30] "Eurocode 1: Actions on structures - Part 1–2: General actions - Actions on structures exposed to fire," vol. 1, no. 2005, p. 61, 2011.
[31] R.R. De Sousa, A.C. Costa, and A.G. Costa, "Metodologia para a Avaliação da Segurança Sísmica de Edifícios Existentes baseada em Análises de Fiabilidade Estrutural," 2019.
[32] RBA, "Regulamento do betão armado," no. 1935–10–16. Decreto-Lei N.o 4036, Lisboa, Portugal, 1935.
[33] REBA, "Regulamento de Estruturas de Betão Armado." Decreto Lei N.o 47723, Lisboa, Portugal, 1967.
[34] REBAP, "Regulamento de Estruturas de Betão Armado e Pré-Esforçado," *Diário da República - I Série N.o 174 - 30 de Julho de 1983*. Decreto-Lei N.° 349-C/83, Lisboa, Portugal, 1983.
[35] "Eurocode 3: Design of steel structures - Part 1–2: General rules - Structural fire design," vol. 1, no. 2005, p. 81, 2011.
[36] "EN 1991–1-2: Eurocode 1: Actions on structures - Part 1–2: General actions - Actions on structures exposed to fire," 1991.
[37] Furtado A, Costa C, Arêde A, Rodrigues H. Geometric characterisation of Portuguese RC buildings with masonry infill walls. Eur J Environ Civ Eng 2016;vol. 20(4):396–411. https://doi.org/10.1080/19648189.2015.1039660.